MAGMA (2004) 16: 246–253
DOI 10.1007/s10334-004-0034-z

RESEARCH ARTICLE

J. F. T. Arnold
F. Fidler
T. Wang
E. D. Pracht
M. Schmidt
P. M. Jakob

Imaging lung function using rapid dynamic acquisition of T_1-maps during oxygen enhancement

Received: 10 September 2003
Accepted: 19 December 2003
Published online: 23 March 2004

J. F. T. Arnold (✉)· F. Fidler · T. Wang
E. D. Pracht · P. M. Jakob
Department of Physics,
University of Würzburg,
97074 Würzburg, Germany
E-mail: jsarnold@physik.uni-wuerzburg.de
Tel.: +49-931-8884922
Fax: +49-931-8885851

M. Schmidt
Department of Pneumology,
University of Würzburg
97074 Würzburg, Germany

Abstract This paper describes imaging of lung function with oxygen-enhanced MRI using dynamically acquired T_1 parameter maps, which allows an accurate, quantitative assessment of time constants of T_1-enhancement and therefore lung function. Eight healthy volunteers were examined on a 1.5-T whole-body scanner. Lung T_1-maps based on an IR Snapshot FLASH technique (TE = 1.4 ms, TR = 3.5 ms, FA = 7 °) were dynamically acquired from each subject. Without waiting for full relaxation between subsequent acquisition of T_1-maps, one T_1-map was acquired every 6.7 s. For comparison, all subjects underwent a standard pulmonary function test (PFT). Oxygen wash-in and wash-out time course curves of T_1 relaxation rate (R_1)-enhancement were obtained and time constants of oxygen wash-in (w_{in}) and wash-out (w_{out}) were calculated. Averaged over the whole right lung, the mean w_{out} was 43.90 ± 10.47 s and the mean (w_{in}) was 51.20 ± 15.53 s, thus about 17% higher in magnitude. Wash-in time constants correlated strongly with forced expired volume in one second in percentage of the vital capacity (FEV_1 % VC) and with maximum expiratory flow at 25% vital capacity (MEF25), whereas wash-out time constants showed only weak correlation. Using oxygen-enhanced rapid dynamic acquisition of T_1-maps, time course curves of R_1-enhancement can be obtained. With w_{in} and w_{out} two new parameters for assessing lung function are available. Therefore, the proposed method has the potential to provide regional information of pulmonary function in various lung diseases.

Keywords Fast imaging · Lung imaging · Oxygen- enhancement · Pulmonary function · T_1-mapping

Introduction

The lung is a complex organ that primarily accomplishes gas transfer. A sufficient oxygen uptake by the blood in the lung is essential. Therefore, the detection of altered lung oxygen uptake is of great importance for clinical diagnosis. In the lung, several pathological conditions are characterized through impaired gas exchange processes. Therefore, to evaluate lung function, one has to address ventilation of the alveoli and diffusion of oxygen into pulmonary capillary blood. For an imaging setting with the aim of regional assessment of pulmonary function, the direct use of oxygen as a contrast agent (CA) is obviously interesting.

Oxygen-enhanced MR imaging of the lung has been performed for the first time by Edelman et al. [1]. T_1-weighted lung images while breathing room air were compared with T_1-weighted lung images while breathing pure oxygen and a significant signal enhancement was demonstrated. Breathing 100% oxygen instead of room

air increases the concentration of dissolved oxygen in venous blood of the lungs by approximately five times [2]. This will shorten the T_1 relaxation time of pulmonary venous blood since dissolved oxygen is weakly paramagnetic [3]. Although there exists another T_1 effect, resulting from the lesser portion of the likewise paramagnetic deoxyhemoglobin while breathing 100% oxygen, it has been shown that this has little bearing on T_1 [4,5]. Thus, since the effect of physically dissolved oxygen on the proton spins of blood water is detected, oxygen transfer can be visualized using oxygen as a CA in MR imaging. Compared to other MRI approaches, which try to assess regional pulmonary function using hyperpolarized noble gas imaging [6,7], this one has the major advantage that only standard hardware for proton imaging is needed. In addition, molecular oxygen is one of the most abundant molecules and widely available. But an obstacle still remains, namely that various mechanisms are potentially responsible for the observed signal changes, such as ventilation, perfusion and diffusion, as has been emphasized in the past [8]. However, recently several investigators have reported that dynamic oxygen-enhanced MRI reflects lung function [9–11]. But, because only relative signal changes are detected in T_1-weighted images, a quantitative assessment of the pulmonary function by this approach is critical, since T_1-weighted sequences strongly depend on the exact data acquisition parameters. In T_1-weighted inversion recovery (IR) experiments, the inversion time (TI) determines the resulting image contrast. The signal after waiting TI will vanish for a certain T_1, which may occur in the range of the lung T_1, if TI isn't chosen appropriately. However, the slope of signal enhancement won't be constant throughout the whole range of the lung T_1 even using an optimized TI [12], since the relative signal intensity is not a linear function of T_1. Therefore, T_1-weighted images demonstrate a different change of relative signals in lungs, which show in fact the same changes in T_1 during oxygen enhancement, but which do not have the same magnitude in their T_1 values, e.g. T_1 changes in one lung from 1200 ms to 1050 ms and from 1000 ms to 850 ms in the other. In this case, although the alterations in T_1 were the same, a different oxygen transfer would be diagnosed by using T_1-weighted images. Therefore, this may probably mimic pathology. As an alternative, we propose to dynamically image lung function with oxygen-enhanced MRI by using T_1 parameter maps. This provides an accurate, quantitative assessment of T_1 relaxation rate (R_1)-enhancement vs. time during inhalation of molecular oxygen, which is unbiased by the intrinsic T_1 of the lung.

The purpose of this study was threefold: first, to develop a method for the rapid dynamic acquisition of T_1-maps, second, to obtain time course curves of R_1-enhancement during switching from room air to 100% oxygen and vice versa and thus to obtain time constants of oxygen wash-in and wash-out and third, to experimentally demonstrate the feasibility of imaging pulmonary function with this approach.

Materials and methods

Imaging experiments were performed using a 1.5-T whole-body imager (Magnetom VISION, Siemens Medical Systems, Erlangen, Germany) with a peak gradient amplitude of 25 mT/m and slew rates of 83 T/m/s. For signal reception a four-element body phased array coil was used in all studies.

Rapid dynamic acquisition of T1-maps

A method for a rapid measurement of the T_1 values in the human lungs at an acceptable spatial resolution has been proposed in the past [13]. The basic imaging technique of this method is a Snapshot version [14] of the Tomrop sequence [15] which was first proposed by Look and Locker [16]. First, the magnetization is inverted by applying a nonselective inversion pulse. The relaxation of the longitudinal magnetization is then detected by a series of 16 Snapshot FLASH images. The relaxation behaviour of the longitudinal magnetization M_z in this inversion recovery (IR) Snapshot FLASH experiment is determined by an effective longitudinal relaxation time T_1^*, that is smaller than T_1 [17]. It has been further shown that M_z approaches M^*, a saturation value that is below the equilibrium value M_0. Thus, the relaxation process is governed by the following equation:

$$M_z(t) = M^* - (M_0 + M^*) \cdot \exp(-t/T_1^*) \quad (1)$$

If the condition $\mathrm{TR} < T_1^*$ holds true, with a repetition time TR, the saturation value M^* of the longitudinal magnetization can be simplified to [17]:

$$M^* = M_0 \cdot T_1^*/T_1 \quad (2)$$

For the evaluation of T_1, a three-parameter fit of image intensities is performed on a pixel-by-pixel basis according to the equation

$$M_z(t) = A - B \cdot \exp(-t/C) \quad (3)$$

where $A = M^*$, $B = M_0 + M^*$ and $C = T_1^*$ [17]. Knowing A, B and C, one can derive M^*, M_0 and T_1^*, and the longitudinal relaxation time T_1 can be calculated after a rearrangement of Eq. (2). However, for a dynamic acquisition of T_1-maps Eq. (1) holds true only if the spin system has again reached the thermodynamic equilibrium before each new inversion pulse occurs. Therefore, to fulfil Eq. (1) a relatively long intermediate delay time Δt, which should be on the order of five times T_1, is required between subsequent T_1-maps. In view of the objective to evaluate fast processes by dynamically acquired T_1-maps, a shortening of this intermediate delay time is strongly desirable. One possible approach to shorten Δt has already been reported [18]. In [18], Deichmann et al. modified the described sequence and applied a 90° saturation pulse directly after the acquisition of a T_1-map. Thereafter the original sequence, starting with the next inversion pulse, followed consecutively after a considerably shorter intermediate delay time Δt. It was further shown how the Eqs. (1) and (3) must be modified in this case to calculate the correct T_1. The major drawbacks of this approach are the need for another radio frequency pulse and, as a consequence of this saturation pulse, the nulling of the longitudinal magnetization. In order to achieve an acceptable amount of longitudinal magnetization before the next T_1-map, a certain waiting time after the saturation pulse is mandatory. Therefore, we propose a more straightforward approach, which has an improved signal-to-noise ratio (SNR) per unit time. We report here the feasibility of the use of the original

sequence without modification and without waiting for the full relaxation for the dynamic acquisition of T_1-maps. The calculations, which must be done to obtain the correct T_1 values, are as follows. After acquisition of a T_1-map, an absolute minimum delay Δt must still be used. After Δt, the magnetization, starting from M^*, has reached the magnetization M_a due to free T_1 relaxation. At this point the next inversion pulse is applied and the next T_1-map acquired. Because M_a was inverted instead of M_0, the relaxation curve which is sampled by the imaging sequence, is given by

$$M_z(t) = M^* - (M_a + M^*) \cdot \exp(-t/T_1^*) \tag{4}$$

A three-parameter fit now determines, on a pixel-by-pixel basis, M^*, M_a and T_1^*. Thus, for calculating T_1 according to Eq. (2), the information about M_0 is missing and must be evaluated. This is done as follows. Following the inversion pulse, if no image acquisition would be done, M_z would reach M^* after the time t_M^* due to free T_1-relaxation. Therefore, M^* is given by

$$M^* = M_0 \cdot (1 - 2 \cdot \exp(-t_{M^*}/T_1)) \tag{5}$$

and M_a is given by

$$M_a = M_0 \cdot (1 - 2 \cdot \exp(-(t_{M^*} + \Delta t)/T_1)) \tag{6}$$

Equations (5) and (6) can be combined to

$$M_0 = \frac{\exp(\Delta t/T_1) \cdot M_a - M^*}{\exp(\Delta t/T_1) - 1} \tag{7}$$

Now, the longitudinal relaxation time T_1 can be obtained by solving the equation system of Eqs. (2) and (7) using a numerical solving routine. The intermediate delay time Δt between subsequent acquisition of T_1-maps must be greater than 0, but in principle Δt can be chosen to be any other value.

Initially, phantom experiments were performed. The phantom consisted of ten cylindrical sample tubes filled with water and different concentrations of the CA Endorem (super paramagnetic iron oxide (SPIO) AMI-25). The different concentrations of SPIO were 0.0250, 0.0231, 0.0213, 0.0194, 0.0175, 0.0156, 0.0138, 0.0119, 0.0100 and 0.0081 mmol/l. Eleven rapid dynamic T_1-maps were acquired to obtain ten T_1-maps where the relaxation of the magnetization started at M_a. These were then compared to ten reference T_1-maps, acquired after an intermediate delay time Δt of several minutes to assure complete relaxation of the spins. The series of rapid dynamic T_1-maps were performed at four different delay times Δt, between 2.1 and 5.1 s.

In vivo experiments

Before performing oxygen-enhanced MRI, we compared our new approach in vivo with the conventional method of measuring T_1. The in vivo test consisted of the acquisition of six rapid dynamic T_1-maps (five experiments in which the relaxation of the magnetization started at M_a) with $\Delta t = 3.1$ s and of five reference T_1-maps with Δt of several minutes. These measurements were performed in the lungs of three healthy volunteers during inspiration and expiration breath-hold (BH) in one volunteer, only during inspiration BH in another one and only during expiration BH in a third. Regions of interest (ROI) were drawn in upper, middle and whole right lung and in upper left lung. In each ROI the average of the T_1 values was calculated.

A series of 59 to 63 T_1-maps was dynamically acquired in eight subjects while breathing room air, switching to 100% oxygen and again switching to room air. All 16 lung images of a T_1-map were obtained during a single breath-hold within 3.6 s. The intermediate delay time Δt was again chosen to 3.1 s, thus one T_1-map was acquired every 6.7 s. Three volunteers were imaged at end-expiratory BH and five at end-inspiratory BH. During the time delay Δt between subsequent T_1-maps, the subjects did exactly one inspiration and one expiration. Two ROIs were drawn in the upper right and whole right lung and the average value of all R_1 values, which were located inside a ROI, was calculated. Thus, a time course curve of R_1-enhancement could be drawn for each ROI. For administration of breathing gas we constructed a breathing system that was non-rebreathing and allowed for fast switching between air and pure oxygen. The flow rate was 15–25 l/min, as was found to be optimal in [19]. The volunteers breathed through the same kind of mouthpiece as employed in the clinical lung function laboratory. Breathing through the nose was avoided by using a nose clamp. The volunteers were placed in supine position and a single coronal slice in the dorsal section of the lung was imaged. The entire experiment took 10–15 min. Informed consent was obtained before each study, with approval of the state ethics committee.

Imaging parameters for Snapshot FLASH imaging in vivo are shown in Table 1. The imaging parameters for the phantom measurements were identical, except that the dynamic approach was performed with four different intermediate delay times Δt. The total acquisition time (TA) for one image was thus 224 ms and the image matrix was zero-filled to 256 × 256. For excitation, a Gaussian-shaped pulse with duration of 384 μs was used. For spin inversion, a nonselective hyperbolic secant pulse with duration of 10.24 ms was applied.

Lung function parameters and comparison to pulmonary function test (PFT)

To obtain parameters for evaluating lung function, the time course curves of the two ROIs were fitted to two exponential curves for each ROI, because oxygen wash-in occurs exponentially [20]. The time course curve was therefore divided into two parts. Directly after switching from air to 100% oxygen, a wash-in curve was fitted and thus a wash-in time constant w_{in} was obtained according to

$$R_1(t) = a + b \cdot (1 - \exp(-t/w_{in})) \tag{8}$$

where a, b are fit parameters and t is the time. For obtaining the wash-out time constant w_{out}, the segment directly after switching from pure oxygen to room air was taken and was fitted with the equation

$$R_1(t) = c + d \cdot \exp(-t/w_{out}) \tag{9}$$

where c and d are fit parameters.

For comparison, the volunteers underwent routine pulmonary function testing. The PFT comprised several examinations on a body plethysmograph, which has an integrated spirometry unit (Masterlab, Jaeger, Wuerzburg, Germany). Several variables of pulmonary function were assessed, including dynamic and static lung volumes, arterialized blood gases and the diffusing capacity. In the comparison between PFT and dynamic MRI, only the dynamic variables of forced expired volume in one second as a percentage of

Table 1 Imaging parameters for Snapshot FLASH imaging in vivo

Method	TE (ms)	TR (ms)	FA^0	Slice thickness (mm)	Matrix	FOV (mm^2)	TA map (s)	Δ t	Start. mag.
Reference	1.4	3.5	7	15	64 × 128	500 × 500	3.6	3 min	M_0
Dynamic	1.4	3.5	7	15	64 × 128	500 × 500	3.6	3.1s	M_a

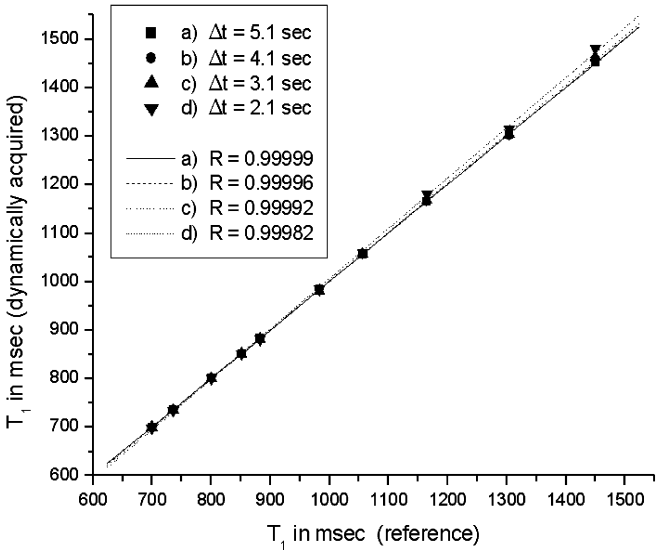

Fig. 1 Results of the phantom measurements are shown. The mean of ten dynamically acquired T_1 values versus the mean of ten reference T_1 values are drawn for ten different sample tubes. For the dynamic acquisition of the T_1 measurements, four different intermediate delay times Δt were studied. For each Δt a linear regression has been made and the squares of the correlation coefficients R^2 of all four lines are approximately 1.000 ($p < 0.0001$). The standard deviation of the T_1 measurements is smaller than the symbols

the vital capacity (FEV_1 % VC) and maximal expiratory flow at 25% of forced vital capacity (MEF25) were used and, in addition, the diffusing capacity of the lung for carbon monoxide (DL_{CO}). DL_{CO} was measured using a steady-state technique [21]. Data were compared with normal standards [22].

Results

Phantom experiments

The results of the described approach on the phantom are shown in Fig. 1. There is excellent agreement of the dynamically acquired T_1 values and the reference T_1 values. The squares of the correlation coefficients R^2 are approximately 1.000 ($p < 0.0001$) and highlight the equality of the T_1 values measured with both methods. The standard deviations of the T_1 measurements are all less than 0.7%. In the case of the largest T_1 value and the smallest Δt of 2.1 s, the highest deviation of 2.15% from the dynamically acquired value 1481.9 ± 9.0 ms to the reference value of 1450.0 ± 1.4 ms was observed. For $\Delta t = 3.1$ s, which was used in all other experiments, the largest deviation from a reference value was 0.3%.

In vivo experiments

All examinations were performed safely and without complications. None of the volunteers reported discomfort and no adverse reactions could be noticed. The intermediate delay time of $\Delta t = 3.1$ s was sufficient to expire and inspire exactly once. As an example, a dynamically acquired T_1-map and a corresponding reference T_1-map is presented in Fig. 2. The position of the diaphragm differs slightly, but the equivalence of the quality of both maps can be clearly seen. Table 2 shows the results of the T_1 measurements in three healthy volunteers. The mean of five dynamically acquired measurements is compared with the mean of five reference measurements from four different ROI and depicts an excellent match of dynamically acquired and reference T_1 values. A correlation of the 16 dynamically acquired T_1 values with their 16 reference values results in a very good correlation coefficient of $R = 0.97$ ($R^2 = 0.95$; $p < 0.0001$). In most cases the standard deviation of the dynamically acquired T_1 values is slightly higher than that of the reference values.

Time course curves of R_1-enhancement in the ROI from upper right and whole right lung of volunteer 7 are displayed in Fig. 3. After 80.4 s the room air was switched to 100% oxygen, after which R_1 increases exponentially and almost reaches a new steady state after 281.4 s, when the oxygen is switched back to room air. R_1

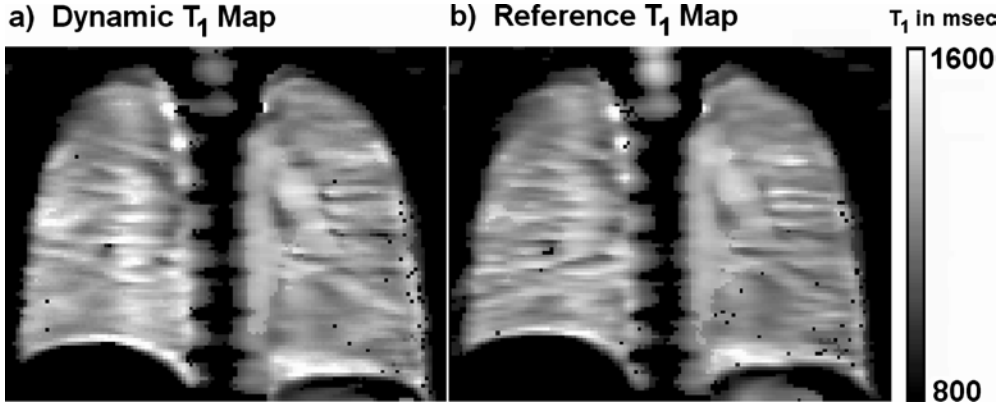

Fig. 2 Grey scaled T_1-maps of human lung are shown and below the left lungs a part of the spleen. **a** One T_1-map out of a series of dynamical acquired maps, with intermediate delay time $\Delta t = 3.1$s. **b** Reference T_1-map, acquired after the magnetization had reached the equilibrium magnetization M_0. Both T_1-maps show equivalent quality

Table 2 Mean dynamic acquired T_1 values and mean reference T_1 values of five measurements in each case in four different ROIs (upper, middle, whole right and upper left lung) are shown in ms for three subjects

Subject	Breath-hold	Mean ± SD			
		ROI 1	ROI 2	ROI 3	ROI 4
1	Exp-dynamic	1224.6 ± 40.0	1297.4 ± 28.8	1299.2 ± 26.7	1241.7 ± 47.5
	Exp-reference	1239.6 ± 13.9	1286.6 ± 10.2	1282.9 ± 8.5	1268.3 ± 17.4
	Insp-dynamic	1123.4 ± 18.3	1243.1 ± 25.6	1210.1 ± 20.1	1129.4 ± 40.7
	Insp-reference	1140.4 ± 13.5	1226.8 ± 37.6	1210.1 ± 33.1	1131.7 ± 26.3
2	Exp-dynamic	1144.1 ± 47.4	1369.1 ± 43.5	1343.2 ± 37.5	1284.2 ± 44.0
	Exp-reference	1172.3 ± 19.2	1396.7 ± 14.1	1367.8 ± 9.2	1300.3 ± 13.2
3	Insp-dynamic	1185.0 ± 23.0	1209.3 ± 11.5	1223.9 ± 9.7	1210.2 ± 11.2
	Insp-reference	1164.3 ± 17.7	1211.0 ± 23.0	1213.6 ± 16.6	1200.3 ± 25.4

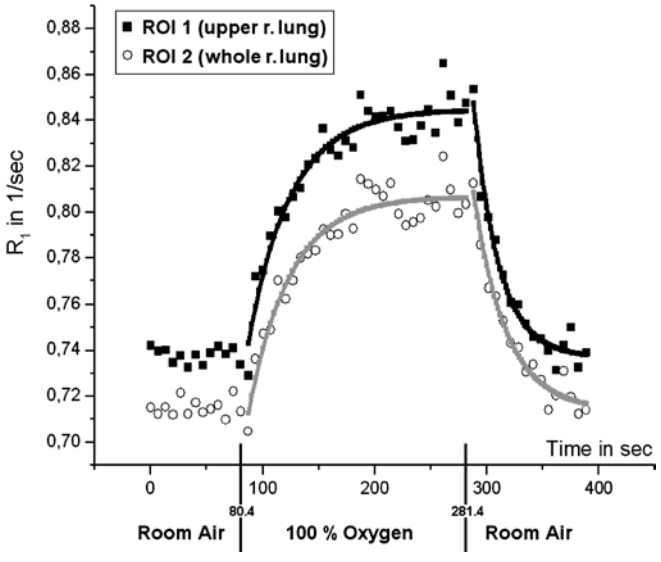

Fig. 3 An example of a time course curve of R_1-enhancement can be seen from the upper and whole right lung of a healthy volunteer. After 80.4 s the room air was switched to 100% oxygen and after 281.4 s gas was switched back to room air. Both time course curves were fitted by two exponential curves, in each case after switching gases. For the upper right lung time constants of wash-in $w_{in} = 38.09 \pm 0.85$ s and of wash-out $w_{out} = 22.63 \pm 2.60$ s were determined. For the whole right lung time constants of wash-in and wash-out were $w_{in} = 36.88 \pm 0.80$ s and $w_{out} = 29.22 \pm 3.86$ s

then starts to decay exponentially back to the baseline. The time constants of wash-in and wash-out of all eight volunteers are listed in Table 3. The overall average of wash-in time constants is 47.21 s in upper and 51.20 s in whole right lung. The overall average of wash-out time constants is 45.79 s in upper and 43.90 s in whole right lung. Thus, wash-in time constants in the upper right lung are on average about 3% and in the whole right lung about 17% higher in magnitude than the wash-out time constants. A significant difference between measurements done in inspiration or expiration BH was not observed, though it seems that the time constants of those time course curves during BH in end-inspiration are slightly greater than those where the BHs were done in end-expiration.

Because routine PFT can only evaluate global lung function, only the time constants of whole right lung were compared with parameters of the PFT. Fig. 4 depicts that FEV_1 % VC (as a percentage of the reference value) correlates strongly with the wash-in time constant w_{in} ($R^2 = 0.82$; $p = 0.00199$), whereas the correlation with the wash-out time constant is suboptimal ($R_2 = 0.33$; $p = 0.13555$). In Fig. 5 an excellent correlation of w_{in} with MEF25 (as a percentage of the reference value) can be seen ($R^2 = 0.91$; $p = 0.00026$) and again a weak correlation of w_{out} with MEF25 ($R^2 = 0.46$; $p = 0.06368$) is visible. Fig. 6 shows a correlation of the DL_{CO} measurements of seven of the volunteers (as a percentage of the reference value) with their time constants, but DL_{CO} correlates with neither w_{in} ($R_2 = 0.00$; $p = 0.93643$) nor w_{out} ($R^2 = 0.18$; $p = 0.33984$). The DL_{CO} measurements of one volunteer had to be discarded, because he had been smoking shortly before the examination, which gave abnormally high DL_{CO} results.

Discussion

The present study demonstrates the potential to image lung function by dynamic acquisition of T_1-maps during oxygen enhancement. A new approach for a rapid dynamic acquisition of T_1-maps was introduced. The T_1 values in the human lung range from 800 ms to 1400 ms [8,19,23,24]. The results of the measurements on a phantom, which consisted of tubes with T_1 in the range of 700–1450 ms, clearly illustrated its feasibility for lung T_1-mapping. In addition, the comparison of the new approach with the reference in vivo showed excellent correlation of the measured T_1 values. Thus, we conclude that T_1 measurements can be measured dynamically and accurately using the new approach.

The T_1 decay time is a fundamental specific property of the tissue. Thus, acquiring quantitative T_1-maps is more precise than simple acquisition of T_1-weighted sequences. With this new rapid dynamic T_1-map acquisition technique, time course curves of R_1-enhancement can be obtained, and, by switching the breathing gas, wash-in and wash-out time constants can be derived.

Table 3 Summary of wash-in and wash-out time constants of upper and whole right lung in eight healthy volunteers. Time constants are given in seconds

Volunteer	Breath-hold	Upper r. lung		Whole r. lung	
		$w_{in} \pm SD$	$w_{out} \pm SD$	$w_{in} \pm SD$	$w_{out} \pm SD$
1	Insp.	83.01 ± 16.57	56.22 ± 15.59	76.24 ± 17.27	52.25 ± 12.19
2	Insp.	33.60 ± 6.88	46.79 ± 25.81	30.69 ± 9.12	35.60 ± 19.82
3	Insp.	43.23 ± 11.25	30.61 ± 11.83	54.61 ± 13.33	32.16 ± 6.92
4	Insp.	41.26 ± 8.17	56.94 ± 25.15	37.68 ± 8.68	42.61 ± 14.54
5	Insp.	47.32 ± 9.87	54.32 ± 12.54	64.03 ± 15.43	50.82 ± 14.44
6	Exp.	43.93 ± 9.98	47.43 ± 18.31	59.74 ± 13.75	51.88 ± 24.15
7	Exp.	38.09 ± 0.85	22.63 ± 2.60	36.88 ± 0.80	29.22 ± 3.86
8	Exp.	47.22 ± 7.17	51.39 ± 2.60	49.73 ± 14.66	56.66 ± 11.07
Mean ± SD	Insp.	49.68 ± 19.28	48.98 ± 11.03	52.65 ± 18.69	42.69 ± 8.93
Mean ± SD	Exp.	43.08 ± 4.62	40.48 ± 15.59	48.78 ± 11.46	45.92 ± 14.66
Mean ± SD	All	47.21 ± 15.18	45.79 ± 12.58	51.20 ± 15.53	43.90 ± 10.47

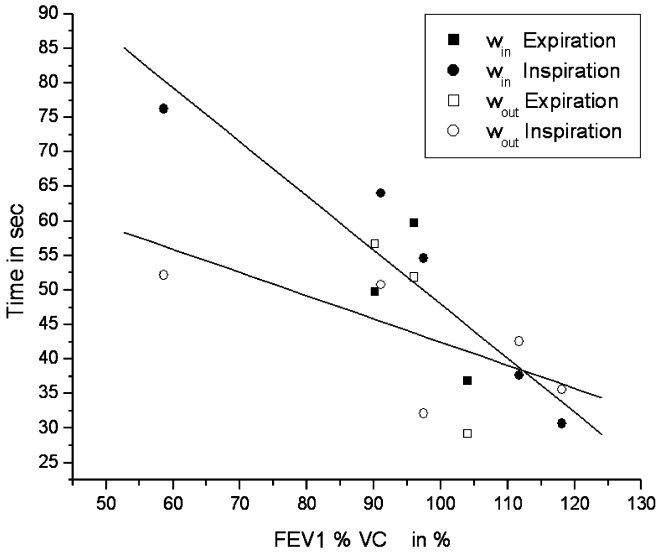

Fig. 4 The graph shows strong correlation between the wash-in time constants of the whole right lung of eight healthy volunteers and their forced expired volume in one second as a percentage of the vital capacity (FEV_1 % VC, percentage predicted). The linear regression model (*black line*) yields a correlation coefficient $R = -0.91$ ($R^2 = 0.82$; $y = -1.05x + 149.50$; $p = 0.00199$). Whereas correlation with the wash-out time constants (*grey line*) is suboptimal ($R^2 = 0.33$; $y = -0.34x + 76.09$; $p = 0.13555$)

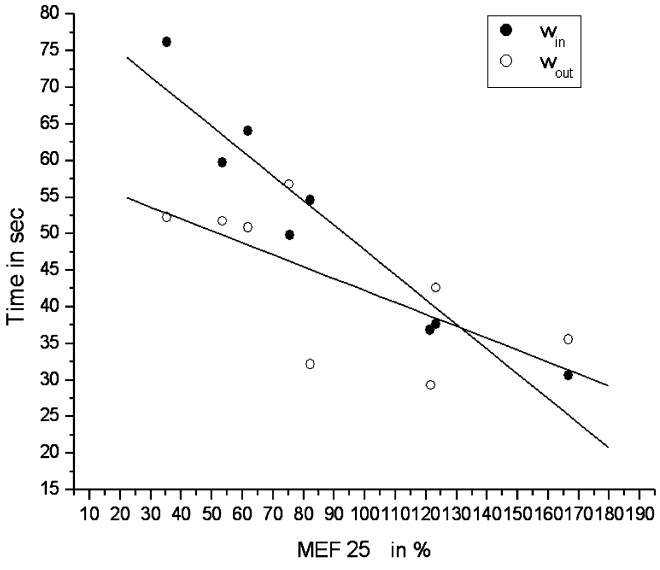

Fig. 5 The graph shows weak correlation between the wash-out time constants of the whole right lung of eight healthy volunteers and their maximum expiratory flow at 25% vital capacity (MEF25, percentage predicted). The linear regression model (*grey line*) yields a correlation coefficient $R = -0.68$ ($R^2 = 0.46$; $y = -2.38x + 214.24$; $p = 0.06368$). Correlation with wash-in time constants (*black line*) is excellent ($R^2 = 0.91$; $y = -0.34x + 81.63$; $p = 0.00026$)

This new approach is clearly favourable compared to dynamic T_1-weighted imaging. In [9,11] linear slopes of signal intensity change were derived. However, oxygen wash-in and wash-out occurs exponentially [20], which can definitely be seen in the time course curves measured in this study. A simplified linear approach, to be tolerant of noisy data, was not needed here, as was proposed in [11].

A slight difference could be measured between mean wash-in and wash-out time constants. The wash-in time constants were found to be greater than w_{out} on average. This may be explained by the contribution of the pulmonary blood flow. Oxygen does not only enter the alveoli by a wash-in process, but also moves out through the alveolocapillary membrane and thus, the pulmonary blood flow works towards wash-out and against wash-in. Another group obtained oxygen wash-in and wash-out by dynamically acquired T_1-weighted images [10]. In accordance with the present work, w_{in} was measured greater than w_{out}, however their time constants were half the magnitude of those seen here. This could be due to two reasons. First, they used a T_1-weighted signal intensity versus time curve instead of a quantitative time course curve of R_1-enhancement for their exponential fitting and second, they measured without BH. In addition in our study the volunteers breathed once for every map obtained for 3.1 s and for 3.6 s they held their breath. Thus, approximately half the time of the entire

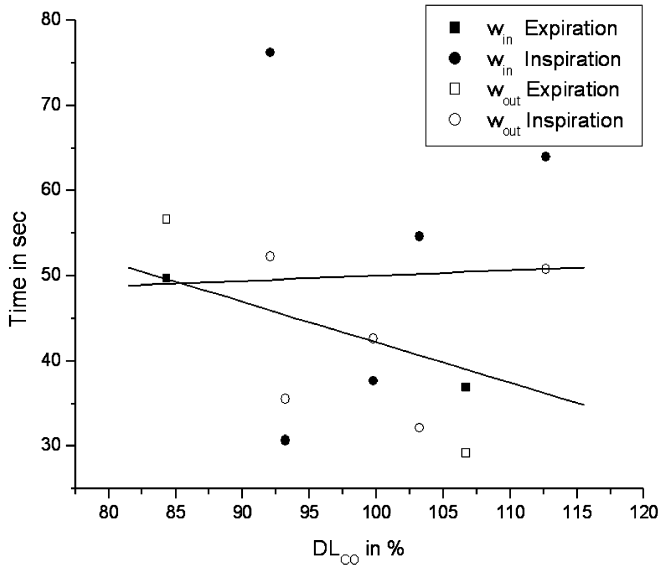

Fig. 6 The graph shows no correlation of the diffusing capacity (DL_{CO}, percentage predicted), neither with the wash-in time constant (*black line*; $R^2 = 0.00$; $y = 0.06x + 43.73$; $p = 0.93643$) nor with the wash-out time constant (*grey line*; $R^2 = 0.18$; $y = -0.47x + 89.65$; $p = 0.33984$) of the whole right lung of seven healthy volunteers

examination the volunteers were breath-holding and therefore, wash-in and wash-out time constants appear to be greater than they should be if breathing were normal. In principle, it is also possible to use the approach of this study to measure time course curves of R_1-enhancement without BH of the volunteers. This would also enable further reduction of the intermediate delay time Δt, since no time for breathing between subsequent T_1-maps is needed. However the T_1-maps acquired without BH may show severe motion artefacts, especially in the lower lobes near the diaphragm. Additionally the T_1 values will differ slightly from their reference values if Δt is very short, as can be seen in the results of the phantom. What is also unclear is the influence of BH position on the time constants. This question cannot be answered by this study due to the low number of volunteers examined.

Comparison of the time constants with parameters of PFT showed good correlation in the case of w_{in}. The correlation of w_{out} with the PFT parameters was only weak. A probable explanation may be inherent to the way the experiment was performed. After switching the breathing gas, the oxygen wash-in was examined for 201s; the wash-out, after another switching, was examined for only 120 s. After these 201 s the oxygen wash-in was nearly completed, whereas the wash-out after 120 s was not (Fig. 3). Thus, the fit for the wash-in time constants could be calculated more accurately than that for the wash-out time constants.

Both parameters, MEF25 and FEV_1 % VC, are strongly related to the ventilation of the subject. Therefore, we conclude that wash-in and wash-out time constants can depict ventilation and pulmonary function. By calculation of pixel-by-pixel maps of wash-in and wash-out time constants, a new tool for a regional assessment of pulmonary function could be developed. Because wash-in and wash-out time constants differ from each other, we gain two new parameters for a MRI-based PFT. However, a correlation between DL_{CO} and R_1-enhancement could not be observed, as was shown between DL_{CO} and signal intensity enhancement in a dynamic T_1-weighted approach by Müller et al. [11]. This contradiction may be explained by the possibility that the T_1-weighted approach may lead to a wrong diagnosis, as was stated in the introduction. Another reason for the discrepancy may be that Müller et al. [11] used a simplified linear fit to signal intensity data, instead of exponential fitting. In addition, it is probable that the patients examined in [11] showed not only a correlation of signal intensity enhancement with DL_{CO}, but also a correlation with MEF25 and FEV_1 % VC. However, the issue of correlation between time constants and PFT ventilation parameters was not explored by Müller et al. [11]

For an assessment of differences in the oxygen uptake in anterior–posterior dimensions, it is necessary to acquire several slices. Although only a single slice was imaged in this study, this is not a major drawback of the new approach. With parallel imaging, for example, it should be possible to acquire three to four slices in an interleaved fashion. In addition, because of the very short time needed for the experiment, it could be easily repeated three times in half an hour. Thus, in half an hour twelve slices could be examined and, therefore, the whole lung could be evaluated.

Volunteers easily cooperated, in particular with the breath-holding pattern. Therefore, our approach provides an easily tolerable method of regional pulmonary function testing. In comparison to ventilation imaging techniques using hyperpolarized gases, only standard ^1H imaging hardware is needed. Compared to other ^1H PFT imaging approaches the quantitative rapid dynamic acquisition of T_1-maps probably has a higher potential for diagnosing lung diseases, especially those related to ventilation defects, and is more accurate than working with T_1-weighted techniques. Further studies using this technique should be performed on patients with regional ventilation defects to explore further the prospect for diagnosing pulmonary diseases with this new approach.

Acknowledgements We would like to thank Karin Kretzer of the pulmonary function lab of the department of pneumology at the University of Würzburg for the performance of the pulmonary function tests.

References

1. Edelman RR, Hatabu H, Tadamura E, Li W, Prasad PV (1996) Noninvasive assessment of regional ventilation in the human lung using oxygen-enhanced magnetic resonance imaging. Nat Med 2:1236–1239
2. Tadamura E, Hatabu H, Li W, Prasad PV, Edelman RR (1997) Effect of oxygen inhalation on relaxation times in various tissues. J Magn Reson Imaging 7:220–225
3. Young IR, Clarke GJ, Bailes DR, Pennock JM, Doyle FH, Bydder GM (1981) Enhancement of relaxation rate with paramagnetic contrast agents in NMR imaging. J Comput Tomogr 5:543–546
4. Brooks RA, Chiro GD (1987) Magnetic resonance imaging of stationary blood: a review. Med Phys 14:905–913
5. Thulborn KR, Waterton JC, Matthews PW, Radda GK (1982) Oxygenation dependence of the transverse relaxation time of water protons in whole blood at high field. Biochim Biophys Acta 714:265–270
6. Gast KK, Puderbach MU, Rodriguez I, Eberle B, Markstaller K, Hanke AT, Schmiedeskamp J, Weiler N, Lill J, Schreiber WG, Thelen M, Kauczor HU (2002) Dynamic ventilation ^{3}He-magnetic resonance imaging with lung motion correction: gas flow distribution analysis. Invest Radiol 37:126–134
7. Markstaller K, Kauczor HU, Puderbach M, Mayer E, Viallon M, Gast K, Weiler N, Thelen M, Eberle B (2002) ^{3}He-MRI-based vs. conventional determination of lung volumes in patients after unilateral lung transplantation: a new approach to regional spirometry. Acta Anaesthesiol Scand 46:845–852
8. Löffler R, Müller CJ, Peller M, Penzkofer H, Deimling M, Schwaiblmair M, Scheidler J, Reiser M (2000) Optimization and evaluation of the signal intensity change in multisection oxygen-enhanced MR lung imaging. Magn Reson Med 43:860–866
9. Ohno Y, Hatabu H, Takenaka D, Adachi S, Van Cauteren M, Sugimura K (2001) Oxygen-enhanced MR ventilation imaging of the lung: preliminary clinical experience in 25 subjects. AJR 177:185–194
10. Hatabu H, Tadamura E, Chen Q, Stock KW, Li W, Prasad PV, Edelman RR (2001) Pulmonary ventilation: dynamic MRI with inhalation of molecular oxygen. EJR 37:172–178
11. Müller CJ, Schwaiblmair M, Scheidler J, Deimling M, Weber J, Löffler R, Reiser M (2002) Pulmonary diffusing capacity: assessment with oxagen-enhanced lung MR imaging – preliminary findings. Radiology 222:499–506
12. Chen Q, Jakob PM, Griswold MA, Levin DL, Hatabu H, Edelman RR (1998) Oxygen enhanced MR ventilation imaging of the lung. MAGMA 7:153–161
13. Jakob PM, Hillenbrand CM, Wang T, Schulz G, Hahn D, Haase A (2001) Rapid quantitative lung 1H T1 mapping. J Magn Reson Imaging 14:795–799
14. Haase A (1990) Snapshot FLASH MRI. Applications to T1, T2 and chemical shift imaging. Magn Reson Med 13:77–89
15. Graumann R, Deimling M, Heilmann T, Oppelt A (1986) A new method for fast and precise T1 determination. SMRM Book of Abstracts 3:922–923
16. Look DC, Locker DR (1970) Time saving in measurement of NMR and EPR relaxation times. Rev Sci Instrum 41:250–251
17. Deichmann R, Haase A (1992) Quantification of T1 values by SNAPSHOT FLASH NMR imaging. J Magn Reson 96:608–612
18. Deichmann R, Hahn D, Haase A (1999) Fast T1 mapping on a whole-body scanner. MRM 42:206–209
19. Mai VM, Liu B, Li W, Polzin J, Kurucay S, Chen Q, Edelman RR (2002) Influence of oxygen flow rate on signal and T1 changes in oxygen-enhanced ventilation imaging. JMRI 16:37–41
20. Comroe JH, Forster RE, Dubois AB, Briscoe WA, Carlsen E (1968) Die Lunge – Klinische Physiologie und Lungenfunktionsprüfungen, 2nd edn. F. K. SchattauerVerlag, Stuttgart
21. Bates, DV, Boucot NG, Dormer AE (1955) The pulmonary diffusing capacity in normal subjects. J Physiol (Lond) 129:237–252
22. Quanjer PH, Tammeling GJ, Cotes JE, Pederson OF, Peslin R, Yernault J (1993) Lung volumes and forced ventilatory flows: report of working party, standardisation of lung function tests. European community for steel and coal – official statement of the European respiratory society. Eur Respir J 6(suppl 16):5–40
23. Mai VM, Knight-Scott J, Edelman RR, Chen Q, Keilholz-George S, Berr SS (2000) 1H magnetic resonance imaging of human lung using inversion recovery turbo spin echo. JMRI 11:616–621
24. Jakob PM, Wang T, Schulz G, Hebestreit H, Hebestreit A, Elfeber M, Hahn D, Haase A (2002) Magnetisation transfer short inversion time inversion recovery enhanced 1H MRI of the human lung. MAGMA 15:10–17